Materials Science-Poland, 37(2), 2019, pp. 257-264
http://www.materialsscience.pwr.wroc.pl/
DOI: 10.2478/msp-2019-0027

Dynamic magnetoelastic properties of $Tb_xHo_{0.9-x}Nd_{0.1}(Fe_{0.8}Co_{0.2})_{1.93}$/epoxy composites

W.C. SHEN, L.L. LIN, C.Y. SHEN, S. XING, Z.B. PAN*

Faculty of Materials Science and Chemical Engineering, Ningbo University, Ningbo 315211, China

$Tb_xHo_{0.9-x}Nd_{0.1}(Fe_{0.8}Co_{0.2})_{1.93}$/epoxy ($0 \leqslant x \leqslant 0.40$) composites are fabricated in the presence of a magnetic field. The structural and dynamic magnetoelastic properties are investigated as a function of both magnetic bias field H_{bias} and frequency f at room temperature. The composites are formed as textured orientation structure of 1–3 type with ⟨1 0 0⟩ preferred orientation for $x \leqslant 0.10$ and ⟨1 1 1⟩-orientation for $x \geqslant 0.25$. The composites generally possess insignificant eddy-current losses for frequency up to 50 kHz, and their dynamic magnetoelastic properties depend greatly on H_{bias}. The elastic modulus (E_3^H and E_3^B) shows a maximum negative ΔE effect, along with a maximum d_{33}, at a relatively low $H_{bias} \sim 80$ kA/m, contributed by the maximum motion of non-180° domain-wall. The 1–3 type composite for $x \geqslant 0.25$ shows an enhanced magnetoelastic effect in comparison with 0 to 3 type one, which can be principally ascribed to its easy magnetization direction (EMD) towards ⟨1 1 1⟩ axis and the formation of ⟨1 1 1⟩-texture-oriented structure in the composite. These attractive dynamic magnetoelastic properties, e.g., the low magnetic anisotropy and $d_{33,max}$ as high as 2.0 nm/A at a low $H_{bias} \sim 80$ kA/m, along with the light rare-earth Nd element existing in insulating polymer matrix, would make it a promising magnetostrictive material system.

Keywords: *magnetostriction; magnetostrictive composite; Laves phase; dynamic magnetoelastic properties; magnetization process*

1. Introduction

Magnetostrictive materials, e.g. Laves phase RFe_2 (R = rare earth) compounds, have been widely used as the main component in sensors, actuators, precise control apparatus, etc. [1, 2]. However, the intrinsic mechanical brittleness and the eddy current losses occurring at higher frequencies are known to restrict their applications. To minimize the restrictions imposed by monolithic RFe_2 alloys, the particulate composites have been developed by integrating alloy particles within a passive polymer matrix to obtain the combination of high toughness and less energy loss. Another advantages of these composites over bulk magnetostrictive alloys are low weight and ease of fabrication [3–7].

Composite and monolithic RFe_2 alloys, based on Terfenol-D ($Tb_{0.27}Dy_{0.73}Fe_2$), are recognized as key magnetostrictive materials, but because they use expensive heavy rare-earth metals Tb/Dy, consequently appear not cost-effective enough for commercial applications. In order to further enable the applicability, the introduction of other rare-earth elements as substitution for Tb/Dy offers economical alternative materials that can be used to fabricate the composites. In the past decade, the development of Laves alloys containing light rare-earth metals has been a hot research topic, wherein Nd was shown as a good substitution element. Nd plays an opposite role in magnetocrystalline anisotropy in comparison with Tb, leading to anisotropic properties for both monolithic alloy and composite. Moreover, $NdFe_2$ has a low magnetocrystalline anisotropy and a large crystal deformation along high-symmetry ⟨1 1 1⟩ axis (denoted as λ_{111}, e.g. ∼3100 ppm at 15 K), accompanied by the easy magnetic direction (EMD) along the ⟨1 0 0⟩ axis other than EMD ⟨1 1 1⟩ for $TbFe_2$ [1, 8–11]. Recently, we have prepared the Nd-containing Laves-phase $Tb_xHo_{0.9-x}Nd_{0.1}(Fe_{0.8}Co_{0.2})_{1.93}$ compounds and epoxy-bonded 1–3 type particulate composites, which had high static and quasi-static magnetoelastic properties at room temperature [12, 13].

*E-mail: panzbnbu@126.com

In the present work, we prepared further 0–3 and 1–3 type polymer composites, focusing on their dynamic magnetoelastic properties and the correlation with macroscopic structure, to gain a more complete physical characterization for related magnetostriction applications.

2. Experimental

Polycrystalline alloys with nominal composition $Tb_xHo_{0.9-x}Nd_{0.1}(Fe_{0.8}Co_{0.2})_{1.93}$ ($0 \leqslant x \leqslant 0.40$) were prepared by non-consumable arc-melting process [12]. The ingots, wrapped in Mo foil, were homogenized at 650 °C for 9 days in an inert atmosphere, and then furnace cooled to room temperature (RT). Subsequently, the ingots were ground into a particulate form with randomly distributed sizes in a range of about 75 μm to 150 μm. To prepare the particulate composites, an epoxy-resin bonding route was used to obtain rod samples [14]. Predetermined quantities of alloy particles and epoxy resin (Araldite LY5210/HY2954), corresponding to a particle volume fraction $V_f \sim 0.3$, were homogeneously mixed in a plastic mold. The composites, classified as the 0–3 type and pseudo-1–3 type, were prepared without and with a curing magnetic field, respectively. The value of the curing magnetic field was kept at 960 kA/m along the longitudinal direction of the mold. As for the 0–3 type composite, the embedded alloy particle phase is isolated and surrounded by the epoxy matrix phase, the epoxy matrix phase is connected in all three directions, while for the 1–3 type, the embedded particles are connected in one direction along the curing field [15]. After solidification at RT, the rod samples were demolded and cut into pieces of dimensions 13 mm in diameter and 20 mm in length.

X-ray diffraction (XRD) with CuKα radiation was employed at RT using a D/max-γA diffractometer equipped with a graphite crystal monochromator. The dynamic magnetoelastic properties were measured in the longitudinal direction of the rod samples with zero pre-stress bias [16, 17]. The DC bias magnetic field H_{bias} was provided by energizing an electromagnet, and the solenoid situated on each pole piece, provided an AC magnetic drive field (H_3). The dynamic strain coefficient d_{33} was obtained from:

$$d_{33} = \frac{S_3}{H_3} \tag{1}$$

where the dynamic magnetostriction S_3 was measured using a lock-in-amplifier and a strain gauge, supplied with a constant current, and magnetic drive field H_3 was acquired using a pick-up coil positioned between the pole pieces. The magnetic flux density B_3 was measured from a search coil wrapped around the composite, and consequently the dynamic relative permeability could be obtained from:

$$\mu_{r33} = \frac{B_3}{\mu_0 H_3} \tag{2}$$

where $\mu_0 = 4\pi \times 10^{-7}$ H/m is the permeability of free space. In this work, H_3 was set to be the amplitude of 1 kA/m with the frequency f sweeping from 1 kHz to 50 kHz, and H_{bias} was controlled in the range of 10 kA/m to 300 kA/m. The dynamic magnetic susceptibility χ_{33} was obtained from $\chi_{33} = \mu_{33} - 1$, accordingly the ratio of the dynamic strain coefficient to the dynamic susceptibility (d_{33}/χ_{33}) was obtained from equation 3 [17]:

$$\frac{d_{33}}{\chi_{33}} = \frac{d_{33}}{\mu_{33} - 1} = \frac{S_3}{M_3} \tag{3}$$

where M_3 is the dynamic magnetization along the longitudinal direction of the rod sample. The elastic moduli at constant magnetic field E_3^H and at a constant magnetic flux density E_3^B were calculated using:

$$E_3^H = 4\rho(Lf_r)^2 \tag{4}$$

$$E_3^B = 4\rho(Lf_a)^2 \tag{5}$$

where L and ρ are the length and density of the composite, respectively. The resonance frequency f_r and anti-resonance frequency f_a were obtained from the curves for the f dependence of μ_{r33}.

3. Results and discussion

XRD analysis confirms that the homogenized $Tb_xHo_{0.9-x}Nd_{0.1}(Fe_{0.8}Co_{0.2})_{1.93}$ alloys are composed essentially of C15 single-Laves phase over the whole concentration range investigated. The XRD patterns for the 0–3 type composite are similar to that of its polycrystalline powders due to the fact that the particles are randomly dispersed in the epoxy matrix. As for the pseudo-1–3 type, wherein XRD performed on the surface was perpendicular to the direction of the curing field, namely, the XRD was carried out along the rod axis parallel to the field, the XRD patterns show the texture preferred orientation. The XRD patterns of the 1–3 type composite, for $x = 0.10$ and 0.25, are shown in Fig. 1. It is seen that the intensities of the ⟨1 1 1⟩-type peaks for $x = 0.25$, such as (1 1 1), (2 2 2) and (3 3 3) peaks, are stronger in comparison with those of 0–3 type, and reflections corresponding to the (1 0 0)-type peaks can be observed for $x = 0.10$, but with no trace of those for 0–3 type.

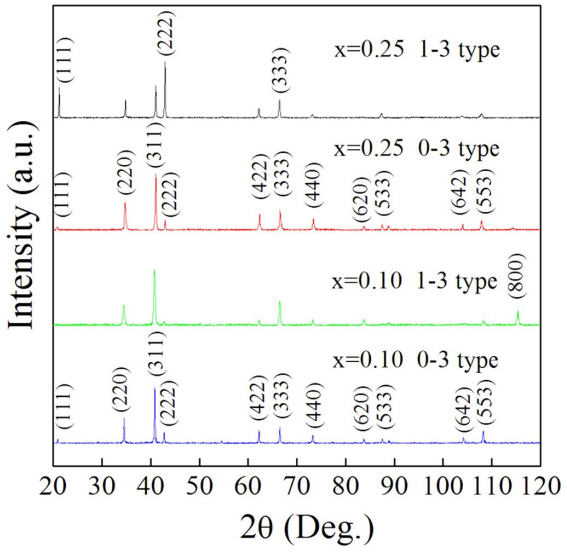

Fig. 1. XRD patterns of the $Tb_xHo_{0.9-x}Nd_{0.1}(Fe_{0.8}Co_{0.2})_{1.93}$ composites ((h k l) of the Laves phase are indexed).

Considering the easy magnetization direction (EMD) for $x \leqslant 0.10$ and $x \geqslant 0.25$ along ⟨1 0 0⟩ and ⟨1 1 1⟩ axis, respectively [12], the composites have been formed as the textured orientation structure, namely, the ⟨1 0 0⟩-oriented structure for $x \leqslant 0.10$ and ⟨1 1 1⟩-oriented one for $x \geqslant 0.25$. This result shows that the presence of a magnetic field is crucial in the fabrication process, as it causes the grains to rotate to ensure their EMD axes along the longitudinal direction of the rod, parallel to the curing field [15].

d_{33} as a function of H_{bias}, at a drive field of 1 kA/m and at a constant frequency of 1 kHz, was measured, and the d_{33}–H_{bias} curves for the 1–3 type $Tb_xHo_{0.9-x}Nd_{0.1}(Fe_{0.8}Co_{0.2})_{1.93}$ composites are shown in Fig. 2. It is seen that all the samples with different Tb content x show similar behavior, that is, d_{33} increases initially and approaches a maximum value at a critical field, and afterward decreases with further increasing H_{bias}, which is typical of all the samples.

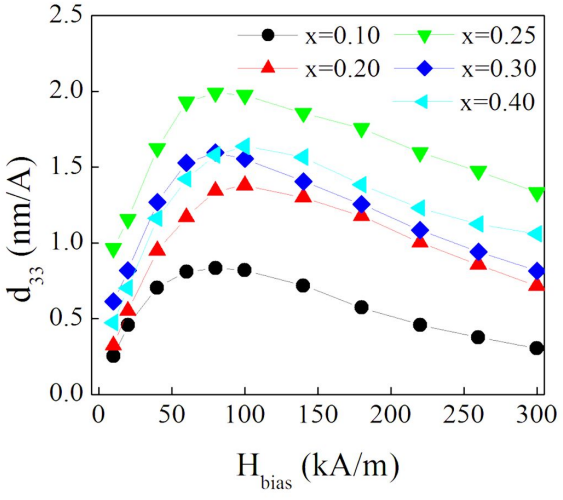

Fig. 2. Magnetic bias field H_{bias} dependence of dynamic strain coefficient d_{33} at 1 kHz for 1–3 type $Tb_xHo_{0.9-x}Nd_{0.1}(Fe_{0.8}Co_{0.2})_{1.93}$ composites.

This variation in the dependence of d_{33} on H_{bias} can be explained by the domain wall movement. It is well established that there exists a considerable amount of magnetic domains and domain walls in the alloy particles, which are mainly classified as 180° and non-180° domains. In the initial technical magnetization process, the magnetization is primarily determined by the 180° domain wall movement due to its relatively easy realization [18, 19]. Subsequently, both 180°

and non-180° domain wall move simultaneously with magnetization process further proceeding upon increasing field. As shown in Fig. 2, d_{33} keeps the small value at a relatively low field due to the more active movement of 180° domain wall, and then it increases with increasing H_{bias}, which can be ascribed to the increase in magnetostriction contributed by the non-180° domain wall motion. d_{33} displays a maximum value at a critical field around $H_{bias} \sim 100$ kA/m, corresponding to the domination of non-180° domains in the technical magnetization process [19, 20]. Thus, it would be not difficult to understand these behaviors for the H_{bias} dependence of d_{33}, considering the fact that the non-180° domain wall motion gives rise to the changes in magnetization with an accompanying magnetostriction, while the 180° domain wall motion only affects the magnetization [19]. In particular, the maximum d_{33} as high as 2.0 nm/A is obtained for the sample with Nd content $x = 0.25$, which is much larger than that for the other compositions. Moreover, $d_{33,max}$ occurs at a relatively low field of $H_{bias} \sim 80$ kA/m, which is smaller than the others, e.g., $H_{bias} \sim 90$ and 100 kA/m for $x = 0.10$ and 0.40, respectively, reflecting its lowest magnetic anisotropy. This behavior is similar to that of its mother alloy, in accordance with the minimum magnetocrystalline anisotropy of the alloy system with $x = 0.25$ [12, 18]. It is believed that d_{33} will be further improved when applied with an additional mechanical stress [5, 21]. Considering the good properties of d_{33}, together with the lowest magnetocrystalline anisotropy and a high low-field static mangetostriction for $x = 0.25$ in monolithic alloy [12], in the following part, our research is focused on the composition of $x = 0.25$.

To better understand the effect of macroscopic composite structure on the magnetoelastic properties, the d_{33} for 0–3 type composites were measured, and the d_{33}–H_{bias} curves for $x = 0.25$ are shown in Fig. 3. It is seen that the maximum d_{33} for 1–3 type composite is much larger than that of the 0–3 type one, which is almost 1.3 times of the latter and approaches 85 % of the polycrystalline alloy.

This enhanced d_{33} effect can be mostly attributed to the formation of ⟨1 1 1⟩-texture-oriented

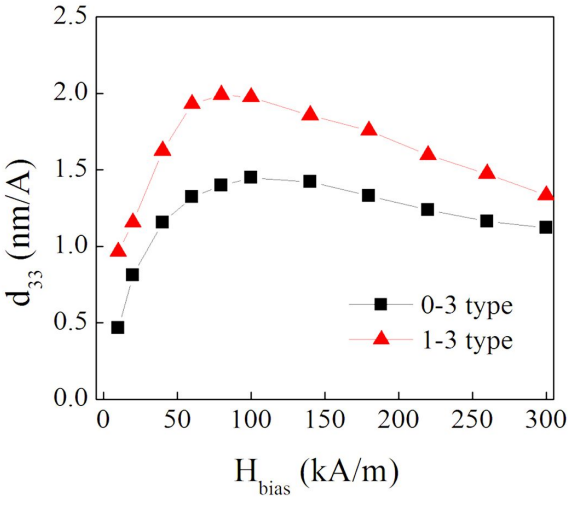

Fig. 3. Magnetic bias field H_{bias} dependence of dynamic strain coefficient d_{33} at 1 kHz for the $Tb_{0.25}Ho_{0.65}Nd_{0.1}(Fe_{0.8}Co_{0.2})_{1.93}$ composites.

structure in 1–3 composite, which can be well understood by the equation for the magnetostriction of a polycrystalline alloy, described as [2, 15]:

$$\lambda = a \cdot \lambda_{111} + (1 - a) \cdot \lambda_{100} \tag{6}$$

where λ_{111} and λ_{100} are spontaneous magnetostriction coefficients of the alloy powders. In the isotropic system, like the polycrystalline alloy and 0–3 type composite, the theoretical value of the coefficient a is 0.60, while for an anisotropic system, such as 1–3 type composite, the value of a is larger than 0.60, owing to its EMD ⟨1 1 1⟩-textured structure, wherein the alloy particles of EMD ⟨1 1 1⟩ lie along the rod axis. As is known, λ_{111} is larger than λ_{100} for the RFe_2 $MgCu_2$-type structure, and in the case of $x = 0.25$, it possesses a large λ_{111}, as high as 850 ppm, while λ_{100} is almost zero [12]. Thus, it is possible that the d_{33}-enhancement effect is achieved for the 1–3 type $Tb_{0.25}Ho_{0.65}Nd_{0.1}(Fe_{0.8}Co_{0.2})_{1.93}$ composite in comparison with the 0–3 type one. In addition, $d_{33,max}$ occurs at a relatively low field of $H_{bias} \sim 80$ kA/m, which is smaller than that of 0–3 type one (∼120 kA/m), reflecting the lower magnetic anisotropy. It can be due to the particle's EMD lying along the rod axis parallel to the measuring magnetic field, which is further proved

by their magnetization processes along the longitudinal and the transverse directions (the magnetization characterization reported in the literature [13]).

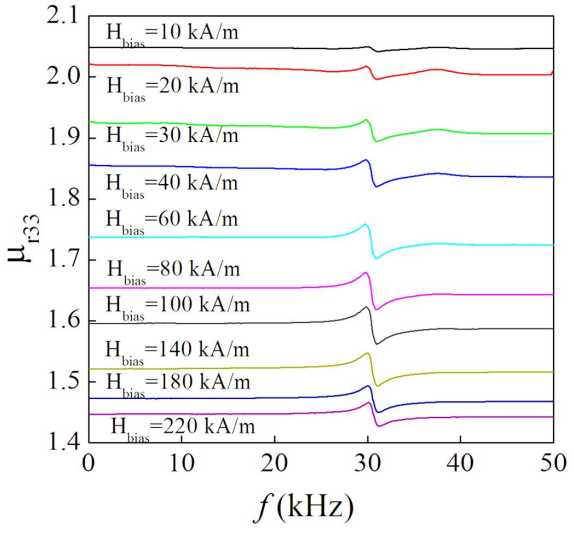

Fig. 4. Frequency f dependence of dynamic relative permeability μ_{r33} at various H_{bias} for the 1–3 type $Tb_{0.25}Ho_{0.65}Nd_{0.1}(Fe_{0.8}Co_{0.2})_{1.93}$ composite.

The f dependence of μ_{r33} for the $Tb_xHo_{0.9-x}Nd_{0.1}(Fe_{0.8}Co_{0.2})_{1.93}$ composites was measured at various H_{bias}, and the μ_{r33} spectra, representing the fundamental longitudinal resonance, are similar for all samples. For clarity, only the μ_{r33}–f curves for 1–3 type $Tb_{0.25}Ho_{0.65}Nd_{0.1}(Fe_{0.8}Co_{0.2})_{1.93}$ composite are shown in Fig. 4. It is evident that μ_{r33} is essentially flat over the whole measured f range of 1 kHz to 50 kHz with no frequency dispersion effect for all H_{bias} levels, except that the longitudinal-mode resonance-induced variations appear around 30 kHz. This mode is of practical interest for longitudinally driven transducers, implying that the eddy-current losses are insignificant in a high frequency up to 50 kHz.

The H_{bias} dependence of μ_{r33} for the 1–3 type $Tb_{0.25}Ho_{0.65}Nd_{0.1}(Fe_{0.8}Co_{0.2})_{1.93}$ composite is presented in Fig. 5, where the values of μ^T_{r33} and μ^S_{r33} are extracted from the μ_{r33}–f curves (Fig. 4) at f = 1 and 50 kHz, respectively. μ^T_{r33} denotes the relative permeability at constant stress,

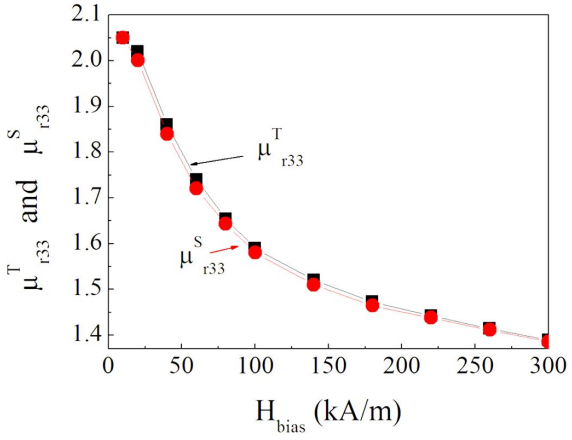

Fig. 5. H_{bias} dependence of μ^T_{r33} and μ^S_{r33} for the 1–3 type $Tb_{0.25}Ho_{0.65}Nd_{0.1}(Fe_{0.8}Co_{0.2})_{1.93}$ composite.

corresponding to the free relative permeability, while μ^S_{r33} denotes the relative permeability at constant strain, which is associated with the clamped relative permeability. We can seen that μ^T_{r33} and μ^S_{r33} reach their maximum values ($\sim$2.05 and $\sim$2.04) at $H_{bias} \sim 10$ kA/m, and then decrease with increasing H_{bias}. The two permeabilities display the maximum at a rather low field, which can be attributed to their relatively easy 180° domain-wall motion. When H_{bias} is increased, the reduced 180° domain wall motion competes with the increased non-180° domain wall motion, leading to a decrease in μ_{r33}. As H_{bias} increases to be around the available maximum field $H_{bias} \sim 300$ kA/m, the permeabilities tend to level off and approach almost the same value, which can be attributed to the approximate saturation in magnetization [18, 22].

The H_{bias} dependence of moduli (E^H_3 and E^B_3) for the 1–3 type $Tb_{0.25}Ho_{0.65}Nd_{0.1}(Fe_{0.8}Co_{0.2})_{1.93}$ composite is plotted in Fig. 6. The two moduli decrease initially with increasing H_{bias}, and then increase with further increasing H_{bias}, exhibiting the minimum values around $H_{bias} \sim 80$ kA/m. In other words, a negative –ΔE effect and a positive –ΔE effect is observed when H_{bias} is less and larger than 80 kA/m, respectively. This behavior of the modulus, i.e., the ΔE effect, is similar to that in an under-pre-stressed monolithic Terfenol-D in which a preferred domain orientation exists,

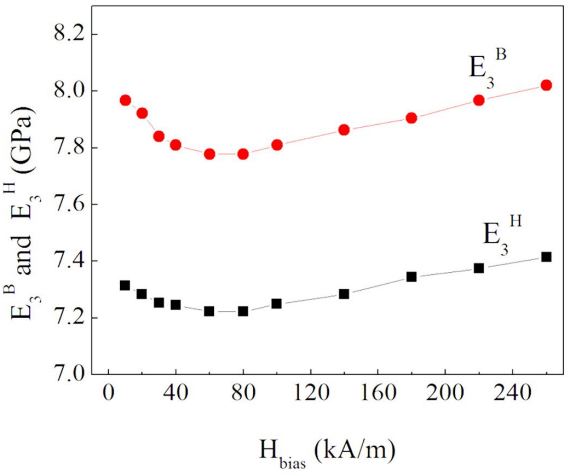

Fig. 6. H_{bias} dependence of E_3^H and E_3^B for the 1–3 type $Tb_{0.25}Ho_{0.65}Nd_{0.1}(Fe_{0.8}Co_{0.2})_{1.93}$ composite.

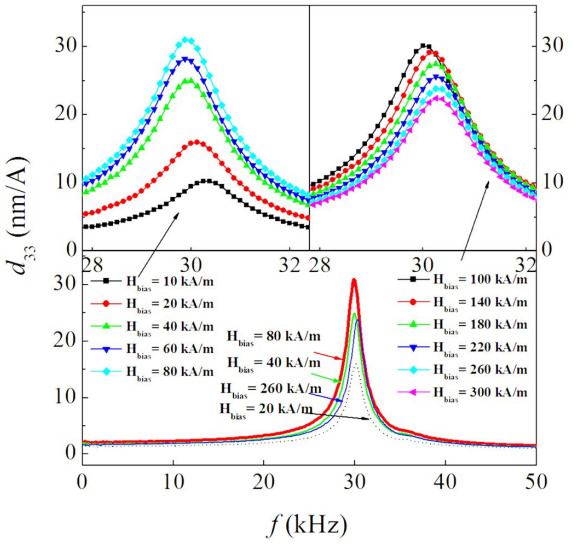

Fig. 7. f dependence of d_{33} at various H_{bias} for the 1–3 type $Tb_{0.25}Ho_{0.65}Nd_{0.1}(Fe_{0.8}Co_{0.2})_{1.93}$ composite. The upper one shows the enlarged central parts of the curves.

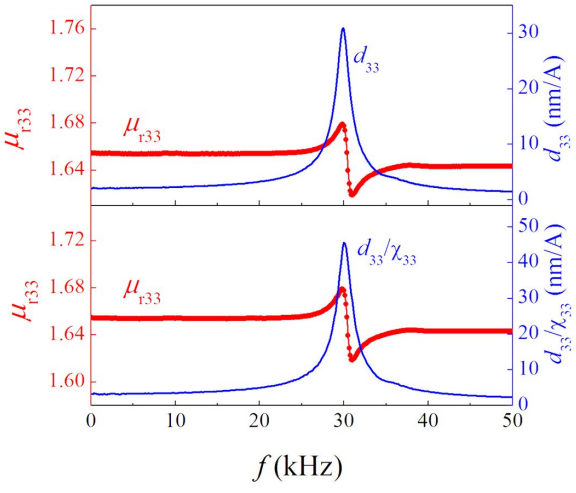

Fig. 8. Resonance and anti-resonance characteristics of μ_{r33}, d_{33} and d_{33}/x_{33} at H_{bias} = 80 kA/m for the 1–3 type $Tb_{0.25}Ho_{0.65}Nd_{0.1}(Fe_{0.8}Co_{0.2})_{1.93}$ composite.

inferring that in the composite, residual stresses due to the epoxy solidification during the fabrication process exist [23]. These stresses create a preferred non-180° domain wall state, which mainly results in the initial decrease in moduli. When H_{bias} increases to around 80 kA/m, the compliance associated with the increased deformation contributed by the non-180° domain-wall motion reaches a maximum, accordingly showing a minimum in stiffness. When H_{bias} increases to above 80 kA/m, the moduli increase with H_{bias}, i.e. the positive –ΔE effect takes place, which is characterized by constraining of non-180° domain-wall motion due to interaction with H_{bias}, and the composite stiffens [18].

The f dependence of d_{33} for the 1–3 type $Tb_{0.25}Ho_{0.65}Nd_{0.1}(Fe_{0.8}Co_{0.2})_{1.93}$ composite at various H_{bias} is presented in Fig. 7. We can see that all the d_{33}–f curves tend to level off with f up to 50 kHz, except that a fundamental resonance mode appears near 30 kHz. The largest d_{33} values are observed at resonance frequency, which are generally 15 times the value at 1 kHz at the same H_{bias} level.

To better illustrate the resonance and anti-resonance characterization, μ_{r33}, d_{33} and d_{33}/x_{33} as a function of f are presented in Fig. 8. It is seen that the resonance frequency f_r in d_{33} accords well with that of μ_{r33}, while the f_r associated with d_{33}/x_{33} coincides with the anti-resonance frequency f_a of μ_{r33}. This frequency dependence character shows a similar variation to that reported by Or et al. [17]. This character is important for such applications, as for example sonar devices and ultrasonic motors, which operate preferably at f_r and at f_a, respectively.

To better understand the effects of M_3 on S_3, the H_{bias} dependence of d_{33}/χ_3 for $H_3 \sim 1$ kA/m at 1 kHz is shown in Fig. 9. It has been established that the ratio d_{33}/χ_{33} is an intrinsic factor that depends only on the intrinsic magnetization parameters, such as direction of magnetic moment, type of domain process and resultant change in magnetostriction [24]. We can see that d_{33}/χ_{33} increases with increasing H_{bias} up to 80 kA/m, and tends to saturate with further increasing H_{bias} to above 80 kA/m.

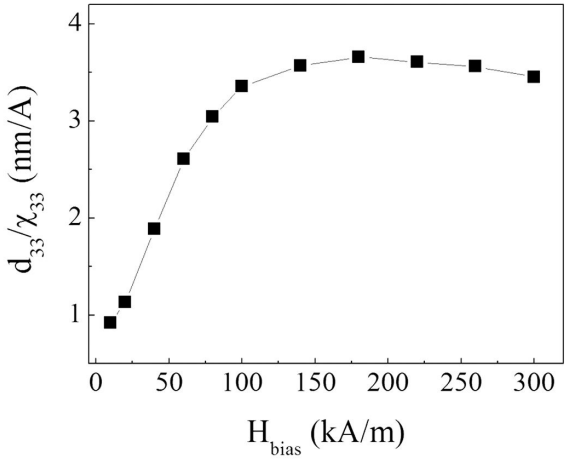

Fig. 9. H_{bias} dependence of d_{33}/x_{33} for $H_3 = 1$ kA/m at $f = 1$ kHz for the 1–3 type $Tb_{0.25}Ho_{0.65}Nd_{0.1}(Fe_{0.8}Co_{0.2})_{1.93}$ composite.

This phenomenon suggests that the dynamic magnetization process can be divided into two regions: below and above the critical $H_{bias} \sim 80$ kA/m. In the initial technical magnetization process, d_{33}/χ_{33} keeps the small values, indicating that the motion of 180° domain wall occurs prior to that of the non-180° one and is dominant in the low field region due to its relatively easy motion, based on its contribution to S_3 but not to M_3. When H_{bias} increases, d_{33}/χ_{33} increases rapidly, which may be ascribed to the fact that the increased motion of non-180° domain walls becomes more active than that of 180° domain walls, in terms of its contribution to both S_3 and M_3. When H_{bias} increases above the critical H_{bias}, both S_3 and M_3 tend to saturate, and consequently the value of d_{33}/χ_3 remains almost constant. In other words, based on equation 3, the change in dynamic magnetostriction is proportional to the change in dynamic magnetization. Similar observation has also been noticed in Terfenol-D/epoxy composite, except that the critical H_{bias} is around 40 kA/m rather than 80 kA/m [17].

4. Conclusions

The texture-oriented $Tb_xHo_{0.9-x}Nd_{0.1}(Fe_{0.8}Co_{0.2})_{1.93}$ 1–3 epoxy/composites with $\langle 1\ 0\ 0\rangle$ orientation preferred for $x \leqslant 0.10$ and $\langle 1\ 1\ 1\rangle$ orientation preferred for $x \geqslant 0.25$, have been fabricated in the presence of a moderate magnetic field. The structural and dynamic magnetoelastic properties were investigated as a function of both H_{bias} and f at room temperature. The composites generally have insignificant eddy-current losses for f up to 50 kHz, and their dynamic magnetoelastic properties depend greatly on H_{Bias}. The elastic moduli (E_3^H and E_3^B) show a maximum negative ΔE effect, along with a maximum d_{33}, at a relatively low $H_{bias} \sim 80$ kA/m, contributed by the maximum motion of non-180° domain-wall. The 1–3 type composite with $x \geqslant 0.25$ shows an enhanced magnetoelastic effect in comparison with 0–3 type, which can be principally ascribed to its EMD along $\langle 1\ 1\ 1\rangle$ axis and forming of $\langle 1\ 1\ 1\rangle$-texture-oriented structure in the composite. These attractive dynamic magnetoelastic properties, e.g. the low magnetic anisotropy and $d_{33,max}$ as high as 2.0 nm/A at a low $H_{bias} \sim 80$ kA/m, along with the light rare-earth Nd element existing in insulating polymer matrix, would make it a promising magnetostrictive material system.

Acknowledgements

This work was supported by the National Natural Science Foundation of China (No. 50801039), Zhejiang Province (Y18E010005), Ningbo City (20191JCGY010115), and K.C. Wong Magna Fund in Ningbo University.

References

[1] CLARK A.E., *Magnetostrictive Rare Earth-Fe_2 Compounds*, in: WOHLFARTH E.P. (Ed.), *Ferromagnetic Materials*, North-Holland, Amsterdam, 1980, Vol. 1, p. 531.

[2] ENGDAHL G., *Handbook of Giant Magnetostrictive Materials*, Academic Press, San Diego, 2000.

[3] ELHAJJAR R., LAW C.T., PEGORETTI A., *Prog. Mater. Sci.*, 97 (2018), 204.
[4] SANDLUND L., FAHLANDER M., CEDELL T., CLARK A.E., RESTORFF J.B., *J. Appl. Phys.*, 75 (1994), 5656.
[5] ALTIN G., HO K.K., HENRY C.P., CARMAN G.P., *J. Appl. Phys.*, 101 (2007), 033537.
[6] MENG H., ZHANG T.L., JIANG C.B., XU H.B., *Appl. Phys. Lett.*, 96 (2010), 102501.
[7] DONG X., QI M., GUAN X., OU J., *Polym. Test.*, 29 (2010), 369.
[8] YIN H.Y., LIU J.J., *Rare Met. Mater. Eng*., 43 (2014), 1275.
[9] RAJASEKHAR P., MARKANDEYULU G., *J. Magn. Magn. Mater.*, 448 (2018), 82.
[10] TANG Y.M., HE Y., HUANG Y., ZHANG L., TANG S.L., DU Y.W., *J. Magn. Magn. Mater.,* 451 (2018), 515.
[11] SONG X.H., LIU J.J., WEI S.H., ZHU X.Y., LI F., ZHANG Z.R., SI P.Z., REN W.J., *Appl. Phys. A.*, 122 (2016), 564.
[12] PAN Z.B., LIU J.J., DU J., REN W.J., *Solid State Commun.*, 211 (2015) 34.
[13] ZHANG Z.R., LIU J.J., SONG X.H., LI F., ZHU X.Y., SI P.Z., *Mater. Sci.-Poland.*, 35 (2017), 81.
[14] PAN Z.B., LIU J.J., LIU X.Y., WANG R., WANG J., SI P.Z., *Int. J. Mod. Phy. B*., 28 (2014), 1450159.
[15] LIU J.J., PAN Z.B., SI P.Z., DU J., *Appl. Phys. Lett*., 103 (2013), 042406.
[16] HUDSON J., BUSBRIDGE S.C., PIERCY A.R., *Sensors Act*., 81 (2000), 294.
[17] OR S.W., NERSESSIAN N., CARMAN G.P., *IEEE Trans. Magn.*, 40 (2004), 71.
[18] LV X.K., OR S.W., LIU W., LIU X.H., ZHANG Z.D., *J. Alloy. Comp.*, 476 (2009), 271.
[19] OR S.W., NERSESSIAN N., MCKNIGHT G.P., CARMAN G.P., *J. Appl. Phys.*, 93 (2003), 8510.
[20] WANG B.W., BUSBRIDGE S.C., GUO Z.J., ZHANG Z.D., *J. Appl. Phys.*, 93 (2003), 8489.
[21] HUDSON J., BUSBRIDGE S.C., PIERCY A.R., *Ferroelectrics*, 228 (1999), 283.
[22] REN W.J., OR S.W., CHAN H.L.W., ZHANG Z.D., *J. Magn. Magn. Mater.*, 293 (2005), 908.
[23] CLARK A.E., RESTORFF J.B., WUN-FOGLE M., LINDBERG J. F., *J. Appl. Phys*., 73 (1993), 6150.
[24] KENDALL D., PIERCY A.R., *IEEE Trans. Magn.*, 26 (1990), 1837.

Received 2018-08-07
Accepted 2019-03-12